Qi *et al. Energy Mater* 2022;2:200035
DOI: 10.20517/energymater.2022.40

Energy Materials

Review

Open Access

Ternary organic solar cells featuring polythiophene

Qingchun Qi[1,2], Huizhen Ke[1,2,3,*], Long Ye[1,*]

[1]School of Materials Science & Engineering, Tianjin Key Laboratory of Molecular Optoelectronic Sciences, Collaborative Innovation Center of Chemical Science and Engineering (Tianjin), Tianjin University, Tianjin 300350, China.
[2]Fujian Key Laboratory of Novel Functional Textile Fibers and Materials, Minjiang University, Fuzhou 350108, Fujian, China.
[3]Fujian Key Laboratory of Electrochemical Energy Storage Materials, Fuzhou University, Fuzhou 350108, Fujian, China.

[*]**Correspondence to:** Prof. Long Ye, School of Materials Science & Engineering, Tianjin Key Laboratory of Molecular Optoelectronic Sciences, Collaborative Innovation Center of Chemical Science and Engineering (Tianjin), Tianjin University, Ya Guan Road 135, Tianjin 300350, China. E-mail: yelong@tju.edu.cn; Prof. Huizhen Ke, Fujian Key Laboratory of Novel Functional Textile Fibers and Materials, Minjiang University, Xi Yuan Gong Road 200, Fuzhou 350108, Fujian, China; Fujian Key Laboratory of Electrochemical Energy Storage Materials, Fuzhou University, Wu Long Jiang Bei Road, Fuzhou 350108, Fujian, China. E-mail: kehuizhen2013@163.com

How to cite this article: Qi Q, Ke H, Ye L. Ternary organic solar cells featuring polythiophene. *Energy Mater* 2022;2:200035. https://dx.doi.org/10.20517/energymater.2022.40

Received: 26 Jul 2022 **First Decision:** 15 Aug 2022 **Revised:** 29 Aug 2022 **Accepted:** 14 Sep 2022 **Published:** 26 Sep 2022

Academic Editors: Yuping Wu, Chunhui Duan **Copy Editor:** Fangling Lan **Production Editor:** Fangling Lan

Abstract

Benefiting from the creation of new photovoltaic materials and innovations in device architectures, organic photovoltaic (OPV) cells are booming. Nonetheless, their prosperity is also accompanied by challenges, such as tedious synthetic routes, increasing costs and insufficient operational stability under practical stresses. Polythiophene, with a simple chemical structure, high scalability and excellent charge transport ability, is expected to be the most promising candidate among all kinds of polymer donors. Ternary mixing, as a simple and effective method for improving the efficiency and stability of OPVs, has attracted significant attention in recent decades. This review provides an overview of the recent advances in ternary OPVs based on polythiophene and discusses the role of various third components in three types of OPV active layers, where polythiophene serves as either the host material or additive, and also clarifies how the third component plays a role in determining morphology and device performance, and finally proposes future research directions for ternary OPVs featuring polythiophene. In short, this review provides insights into polythiophene-based multicomponent systems and helps readers better understand the relationships between morphology, efficiency and stability.

Keywords: Ternary organic solar cells, third components, polythiophene, morphology, efficiency, stability

INTRODUCTION

The increasing demand for energy sources and the continuous aggravation of environmental pollution compel us to seek alternative energy technologies to replace conventional fossil materials. Solar energy, as an inexhaustible and renewable energy source, is essential to this challenge. Organic solar cells (OSCs) demonstrate significant potential for the Internet of Things, electronic devices and portable and wearable sensors due to their merits of lightweight, flexibility and solution processibility[1-4]. Recent decades have witnessed rapid developments in OSCs. For instance, Wang *et al.* recently designed and synthesized three regioregular benzodithiophene-based polymer donors, namely, PBDTT, PBDTT1Cl and PBDTT2Cl[5]. The weak intramolecular charge transfer affords these polymers with large optical bandgaps. PBDTT1Cl-based OSCs gave the best device performance with an impressive power conversion efficiency (PCE) of 17.0%, which could be attributed to the ordered molecule stacking, balanced charge mobility and efficient charge transport. The PCE of single-junction OSCs has now exceeded 19%[6-9], which is already approaching the commercialization application requirements. There is no doubt that the optimization of molecular structure and the improvement of device processing methods play critical roles[10-12]. However, several problems, such as more and more complicated molecular structures, tedious purification processes and increasing costs, also arise as a result. Herein, the design and synthesis of low-cost and high-efficiency photovoltaic materials are urgent for the development of OSCs.

Polythiophene (PT) has always been considered as the most promising polymer donor to be scaled up due to its straightforward synthesis, relatively high crystallinity and excellent batch reproducibility[13-17]. Figure 1 summarizes the chemical structures of PT and its derivatives featured in this article. Among them, poly(3-alkylthiophene) (P3HT) is the most representative material. Acceptors, such as fullerene and its derivatives, have dominated the development of OSCs for a long time due to their advantages of relatively high electron affinity, excellent charge transfer characteristics and good compatibility with polymer donors[18]. As the classic blend system, the photovoltaic properties of P3HT:fullerene have been systemically investigated. Nonetheless, the efficiency of P3HT and fullerene is much lower than that of donor-acceptor-based conjugated polymers because of the intrinsic excessively high-lying energy levels of P3HT and the weak absorption in the visible region of fullerene derivatives[19]. Therefore, downshifting the energy levels of PT by introducing electron-withdrawing substituents and developing acceptors with matched energy levels, complementary absorption and excellent compatibility is critical for promoting the development of PT-based OSCs.

The emergence of non-fullerene acceptors has revived PT-based OSCs. Holliday *et al.* developed a pair of non-fullerene acceptors named O-IDTBR and O-IDFBR in 2016, boosting the efficiency of OSCs based on PT to 6.4%[20]. In 2019, Xu and coworkers[21] designed a novel acceptor matching P3HT, namely, TrBTIC. TrBTIC exhibited excellent solubility in common solvents. They found that the phase separation degree could be well controlled by changing the aging time of P3HT in a green solvent, namely, 1,2,4-trimethylbenzene. Consequently, the device performance was improved from 6.62% to 8.25% after aging for 40 min. The efficiency of PT-based OSCs has been refreshed again since the development of a new Y-series acceptor known as ZY-4Cl[22]. Compared with BTP-4Cl, ZY-4Cl exhibited appropriate phase separation due to the limited miscibility with P3HT. As a result, devices based on P3HT:ZY-4Cl achieved a high efficiency of 9.46% with an improved open-circuit voltage (V_{oc}) of 0.88 V, a short-circuit current density (J_{sc}) of 16.49 mA/cm^2 and fill factor (FF) of 0.65. Recently, our group demonstrated that the crystalline order of these photovoltaic materials could be manipulated by varying the annealing time[23]. Thus, the P3HT:ZY-4Cl blend gave a significantly improved PCE of 10.7% after annealing at 130 °C for 30 s.

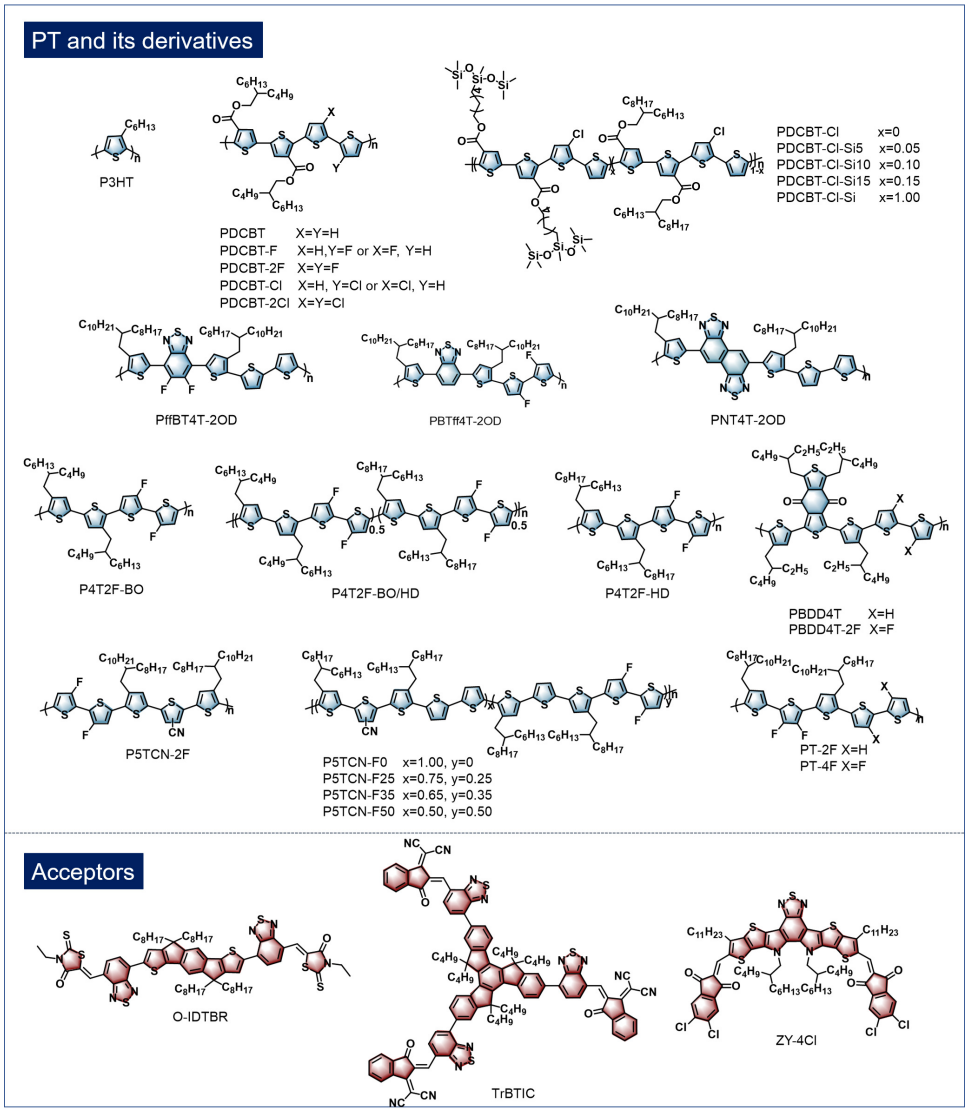

Figure 1. Chemical structures of PT, PT derivatives and non-fullerene acceptors featured in this review.

PT derivatives demonstrate excellent potential for realizing low-cost and highly efficient OSCs[24-28]. An alkoxycarbonyl-functionalized PT derivative known as PDCBT was developed by Zhang *et al.*[29], which exhibited better performance compared with P3HT, either paired with fullerene or non-fullerene acceptors[30]. Since then, a series of studies focusing on PT derivatives have been carried out, contributing to the in-depth understanding of the molecular design and device processing technologies of PT-based OSCs[31-34]. Jia and colleagues[35] reported a series of fluorinated PT derivatives (P4T2F-BO, P4T2F-BO/HD and P4T2F-HD) in 2019. Among all the three polymers, P4T2F-HD gave the highest PCEs of 6.3% and 7.0% when combined with $PC_{70}BM$ and O-IDTBR, respectively. Shortly afterwards, the authors systematically investigated the effect of backbone fluorination degree on the photovoltaic performance of PT-based OSCs[36]. P6T-F100, with the highest fluorination degree, demonstrated enhanced exciton dissociation efficiency and reduced charge recombination and gave the best device performance. Yuan and coworkers[37] constructed a series of high-efficiency OSCs based on PT by designing a cyano group-substituted P5TCN-2F paired with Y-series acceptors. The incorporation of the cyano group not only deepened the energy levels of PT but also enhanced the interchain interaction and polymer crystallinity. As a result, the P5TCN-

2F:Y6-based device achieved a champion PCE of 16.1%, which was much higher than those of previously reported PT-based OSCs. There is no doubt that these successful explorations have laid a solid foundation for the practical application of OSCs.

To further increase the efficiency and improve the stability of OSCs, various methods have been proposed[38,39]. Ternary OSCs have attracted increasing attention in the past decade due to their simple device fabrication process[40-42]. The third component in the form of quantum dots, dye molecules[43], insulating polymers[44], polymer/small molecule donors[45] and fullerene/non-fullerene acceptors[46] is incorporated into the binary systems to form complementary absorption, matched energy levels with host photovoltaic materials or acquire appropriate morphology. Recent advances in ternary OSCs based on non-fullerene acceptors have been clarified, while reviews focusing on PT-based ternary OSCs are still deficient. Therefore, this review aims to summarize the up-to-date advances of PT-based ternary OSCs with the category of application of third components, including quantum dots, insulating polymers, small molecules, fullerene derivatives and polymer donors in fullerene, non-fullerene and polymer acceptors systems. Furthermore, the role of the third component in different systems is also stressed from the perspective of light harvesting, energy transfer, charge transfer and morphology control[47,48]. Figure 2 summarizes the recent advances in polythiophene-based ternary OSCs and the content of this review is depicted in Figure 3.

PT:FULLERENE-BASED TERNARY OSCS

PT:quantum dot:fullerene systems

Quantum dot (QD) solar cells have attracted increasing attention in recent decades due to their advantages of low cost, tunable energy levels and strong light absorption capacity[49]. Research has demonstrated that QDs can effectively extend light absorption and improve the charge transfer of OSCs, contributing to enhanced device performance. The photovoltaic parameters of PT:fullerene-based OSCs with and without QDs are summarized in Table 1. Park and coworkers[50] investigated the effect of ligand type on the performance of P3HT:$PC_{61}BM$:CdSe-based ternary OSCs by introducing two CdSe nanoparticles capped with different ligands, namely, pyridine and fatty acid-oleic acid, into the active layers. Both CdSe nanoparticles had positive effects on the efficiency of OSCs but with different mechanisms. The aggregation of pyridine CdSe nanoparticles in the active layer provided enhanced charge transport pathways, leading to an increased V_{oc}. The morphology of P3HT:$PC_{61}BM$, however, was almost unchanged after incorporating CdSe nanoparticles capped with the small-sized oleic acid. The enhanced PCE of P3HT:$PC_{61}BM$:CdSe capped with oleic acid was ascribed to the increased J_{sc}. In addition to the common semiconductor nanoparticles, such as PbS and CdSe, Si nanoparticles also can be applied in OSCs as the third component. Zhao *et al.* improved the efficiency of P3HT:$PC_{61}BM$ by a factor of 1.4 with 5% $PC_{61}BM$ replaced by Si nanoparticles[51]. Nonetheless, ternary OSCs with P3HT partially being substituted demonstrated a decreased PCE. The difference originated from the better absorption of Si nanoparticles in the short wavelength region compared with $PC_{61}BM$.

Fan and coworkers[52] demonstrated that the incorporation of 2 mg/mL of carbon QDs provided additional carriers at the donor-acceptor interface and a further increase in the carbon QD content resulted in enhanced defects in the active layer. Compared with fullerene and its derivates, QDs exhibit broader spectral absorption and more appropriate energy levels. Substituting fullerenes with small amounts of QDs contributes to enhanced spectral response and reduced charge recombination, leading to increased device performance. Despite these positive effects, the complex purification process and the relatively low yield of QDs restrict their large-scale application in OSCs.

Table 1. Photovoltaic parameters of PT:fullerene-based OSCs with and without QDs

System	Binary system				quantum dot	Ternary system				Ref.
	V_{oc} (V)	J_{sc} (mA cm^{-2})	FF	PCE (%)		V_{oc} (V)	J_{sc} (mA cm^{-2})	FF	PCE (%)	
P3HT:$PC_{61}BM$	0.62	7.35	0.59	2.74	CdSe	0.64	7.50	0.61	2.96	[50]
P3HT:$PC_{61}BM$	0.59	9.14	0.54	2.93	Si NCs	0.57	16.15	0.47	4.11	[51]
P3HT:$PC_{61}BM$	0.53	14.90	0.32	2.50	CQDs	0.55	18.90	0.32	3.32	[52]
P3HT:$PC_{61}BM$	0.36	6.31	0.34	0.78	PbS	0.45	7.88	0.32	1.15	[53]
P3HT:$PC_{61}BM$	/	9.30	0.55	3.08	$BaTiO_3$	/	9.55	0.56	3.27	[54]
P3HT:$PC_{70}BM$	0.61	7.69	0.51	2.39	PbSSe	0.55	9.26	0.48	2.40	[55]
P3HT:$PC_{61}BM$	0.56	4.56	0.51	1.28	CdSe	0.55	5.21	0.53	1.53	[56]
P3HT:$PC_{61}BM$	0.57	10.30	0.52	3.09	NGQD7	0.57	11.60	0.58	3.79	[57]
					NGQD8	0.57	11.40	0.57	3.69	
					rGQD	0.57	11.00	0.56	3.52	
P3HT:$PC_{60}BM$	0.57	8.77	0.50	2.51	CrO_3	0.59	9.94	0.63	3.67	[58]
P3HT:$PC_{61}BM$	0.59	9.51	0.53	2.96	GQDs	0.60	12.31	0.56	4.13	[59]
P3HT:$PC_{61}BM$	0.58	3.47	0.40	0.81	NCs-EHT	0.52	6.34	0.48	1.60	[60]

OSCs: Organic solar cells; QDs: quantum dots; PCE: power conversion efficiency.

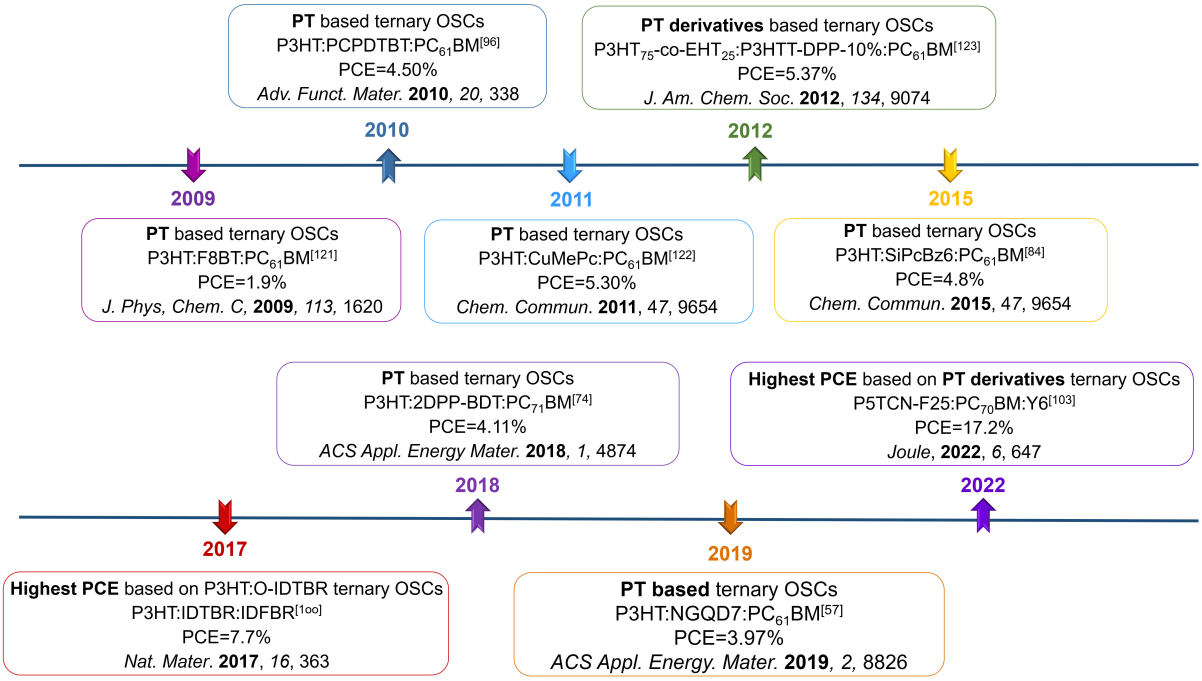

Figure 2. Development of polythiophene-based ternary OSCs. Milestone studies are marked in the boxes[121-123].

PT:insulating polymer:fullerene systems

Insulating polymers, such as commodity plastics, elastomers and resins, have been introduced into OSCs to improve their efficiency, stability and flexibility by controlling the film morphology or forming buffer layer by self-organization. Table 2 summarizes the photovoltaic parameters of PT:fullerene-based OSCs with and without insulating polymers. Ferenczi and coworkers[68] demonstrated that the incorporation of semicrystalline insulators, such as high-density polyethylene (HDPE) and isotactic polystyrene (i-PS), was favorable for the formation of interpenetrated networks under lower fractions, leading to an increased J_{sc}. OSCs with 50% HDPE or i-PS achieved comparable efficiency but increased the active layer thickness,

Table 2. Photovoltaic parameters of PT:fullerene-based OSCs with and without insulating polymers

System	Binary system				Insulating polymer	Ternary system				Ref.
	V_{oc} (V)	J_{sc} (mA cm^{-2})	FF	PCE (%)		V_{oc} (V)	J_{sc} (mA cm^{-2})	FF	PCE (%)	
P3HT: $PC_{61}BM$	0.39	4.01	0.50	0.78	PMMA	0.39	5.40	0.52	1.10	[61]
PffBT4T: $PC_{61}BM$	0.75	17.00	0.73	9.24	TP-C_6	0.75	18.40	0.72	9.41	[62]
P3HT: $PC_{61}BM$	0.59	12.12	0.56	3.97	PEG	0.59	12.67	0.57	4.24	[63]
P3HT: $PC_{61}BM$	0.61	9.92	0.50	3.03	PVP	0.61	13.04	0.49	3.90	[64]
P3HT: $PC_{61}BM$	0.59	8.80	0.56	2.90	P3HT-b-P3FAT	0.60	11.30	0.65	4.40	[65]
P3HT: $PC_{61}BM$	0.56	7.99	0.54	2.40	PVDF	0.56	8.63	0.63	3.07	[66]
P3HT: $PC_{61}BM$	0.57	8.31	0.65	3.05	PDMS-b-PMMA	0.61	8.68	0.67	3.56	[67]

OSCs: Organic solar cells; PCE: power conversion efficiency.

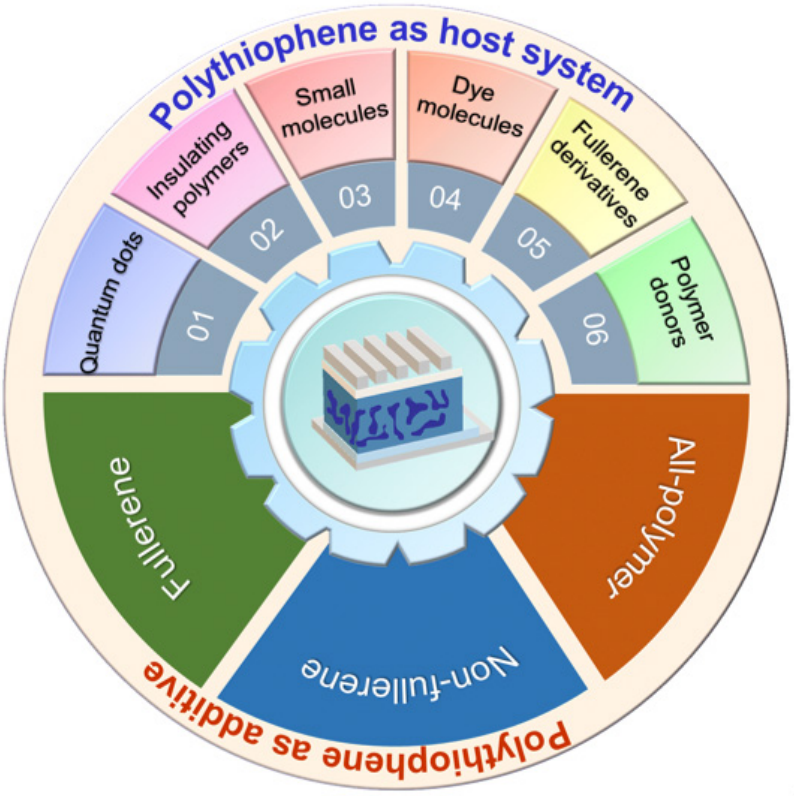

Figure 3. Structure of this review.

which facilitated the large-scale preparation of OSCs. Dauzon and colleagues[69] systematically investigated the effect of two approaches, namely, crosslinking and blending, on the mechanical properties of OSCs. Three crosslinkers ($C_{12}N_3$, PEG_3N_3 and PEG_nN_3) with different polarities and chain lengths and two elastomers with different net types, i.e., polystyrene-block-poly(ethylene-ran-butylene)-block-polystyrene (SEBS) and poly(dimethylsiloxane) (PDMS) were incorporated into the P3HT:$PC_{61}BM$ blends. The bis-azide molecules reacted selectively with $PC_{61}BM$ and suppressed the crystallization of acceptor under thermal stress, contributing to a uniform morphology. Nonetheless, blend films with a SEBS and PDMS weight ratio over 50% exhibited severe phase separation resulting from poor miscibility. Compared with ternary OSCs based on SEBS and PDMS, the efficiency of bis-azide molecules crosslinked devices could be well retained due to the enhanced aggregation of P3HT. Active layers crosslinked with bis-azide molecules

or blended with SEBS demonstrated improved mechanical properties originating from the softening effect induced by the plasticization or the low interaction. Notably, the application of SEBS could be extended to non-fullerene blends, demonstrating excellent potential in the field of flexible electronic devices.

In addition to forming uniform three-phase blend systems, functionalized insulating polymers incorporated into the active layers can also act as the buffer layer due to the surface energy or chemical interaction. Yamakawa *et al.* developed a simple approach to improve the efficiency of P3HT:$PC_{61}BM$ with a low surface energy insulator poly(dimethyl-siloxane)-block-poly(methyl methacrylate) (PDMS-b-PMMA)[67]. The PDMS-b-PMMA segregated at the active layer, self-organized to the buffer layer during the spin-coating process and suppressed the charge recombination between active layer and electrode, with the PCE of P3HT:$PC_{61}BM$ increasing from 3.05% to 3.56%. Yu and coworkers[66] improved the device performance of P3HT:$PC_{61}BM$ by employing a nonvolatile processing additive polyvinylidene fluoride (PVDF). The addition of PVDF improved the absorption in the range of 300-600 nm and enhanced the phase separation of active layer, resulting in improved light-harvesting capacity and interfacial contact. Insulating polymers demonstrate excellent potential for improving the efficiency, thermal stability and mechanical properties of OSCs and the incorporation of commercialized insulating polymers can also reduce the cost of device preparation. Some studies have reported that insulating polymers with a glass transition temperature (T_g) lower than the annealing temperature during device fabrication facilitate the enhancement of PCE since the film morphology can be easily manipulated, while insulating polymers with T_g over the annealing temperature generally have a negative influence on the device performance. Nevertheless, circumstances that employ high-temperature resistant resins as the third component to improve the efficiency of OSCs are not uncommon. Therefore, clarification of the mechanism of insulating polymers affecting the efficiency of OSCs and the construction of the selection principle of the third component are urgently required.

PT:small molecule:fullerene systems

The application of small molecules, including small molecule donors, non-fullerene acceptors and dye molecules, in polythiophene OSCs is featured in this section. Table 3 summarizes the photovoltaic parameters of PT:fullerene-based OSCs with and without conjugated small molecules. Zhang *et al.* systemically investigated the effect of crystallinity of non-fullerene acceptors on the microstructure and photovoltaic performance of PT:fullerene-based OSCs[70]. Two non-fullerene acceptors with different crystallinity, namely, EH-OIDTBR and O-IDTBR, were incorporated into the P3HT:$PC_{71}BM$ blend separately. Ternary blends with both EH-OIDTBR and O-IDTBR demonstrated extended absorption band and enhanced absorption intensity at 602 nm, corresponding to the improved π-π interaction of P3HT. Furthermore, the addition of EH-OIDTBR and O-IDTBR provided more charge transport pathways. Compared with the P3HT:$PC_{71}BM$:EH-OIDTBR ternary blend, the P3HT:$PC_{71}BM$:EH-OIDTBR-based system exhibited smoother morphology, which originated from the more ordered structure of O-IDTBR. Furthermore, the coherent length of P3HT increased with increasing O-IDTBR weight ratio. Both ternary OSCs based on EH-OIDTBR and O-IDTBR achieved an improved average efficiency (4.05% and 4.01%, respectively), which could be attributed to the increased FF and J_{sc}, respectively. Accordingly, the enhanced charge transport efficiency and more balanced electron and hole mobility were responsible for the increased J_{sc} and FF.

Apart from small molecular donors and non-fullerene acceptors, dye molecules are another important component for improving the light-harvesting capacity. The device performances of PT:fullerene-based OSCs with and without dye molecules are listed in Table 4 Honda and coworkers[79] reported a ternary OSC based on P3HT:PCBM:SiPc with enhanced device performance. The ternary blend films exhibited similar absorption before and after annealing, with the maximum absorption peaks at ~460 and ~670 nm, indicating the identical aggregation behavior of P3HT. As expected, the ternary OSCs achieved a PCE of

Table 3. Photovoltaic parameters of PT:fullerene-based OSCs with and without conjugated small molecules

System	Binary system				Conjugated small molecule	Ternary system				Ref.
	V_{oc} (V)	J_{sc} (mA cm^{-2})	FF	PCE (%)		V_{oc} (V)	J_{sc} (mA cm^{-2})	FF	PCE (%)	
P3HT:$PC_{71}BM$	0.60	9.10	0.60	3.30	EH-IDTBR	0.59	10.86	0.63	4.05	[70]
					O-IDTBR	0.59	10.93	0.62	4.01	
P3HT:$PC_{61}BM$	0.62	8.91	0.68	3.77	TT-TTPA	0.62	10.30	0.67	4.26	[71]
P3HT:$PC_{71}BM$	0.57	8.47	0.62	3.00	p-DTS$(FBTTH_2)_2$	0.62	9.35	0.64	3.71	[72]
P3HT:$PC_{61}BM$	0.56	7.54	0.67	2.84	SMA1	0.65	8.00	0.70	3.70	[73]
P3HT:$PC_{71}BM$	0.57	8.80	0.59	2.98	2DPP-BDT	0.59	11.90	0.55	3.80	[74]
P3HT:$PC_{61}BM$	0.53	10.50	0.54	3.00	DPP4T-Cz	0.56	12.90	0.56	4.04	[75]
P3HT:$PC_{61}BM$	0.55	7.05	0.66	2.58	BTT-OT-ORD	0.57	8.25	0.67	3.13	[76]
P3HT:$PC_{61}BM$	0.53	7.53	0.61	2.45	BTT-OT-OTZDM	0.56	7.45	0.62	2.65	
P3HT:$PC_{61}BM$	0.64	7.03	0.46	2.07	*p*-DPP-PhCN	0.66	7.30	0.51	2.48	[77]
P3HT:$PC_{61}BM$	0.58	10.40	0.57	3.44	DH4T	0.60	11.21	0.62	4.17	[78]

OSCs: Organic solar cells; PCE: power conversion efficiency.

Table 4. Photovoltaic parameters of PT:fullerene-based OSCs with and without dye molecules

System	Binary system				Dye molecule	Ternary system				Ref.
	V_{oc} (V)	J_{sc} (mA cm^{-2})	FF	PCE (%)		V_{oc} (V)	J_{sc} (mA cm^{-2})	FF	PCE (%)	
P3HT:$PC_{61}BM$	0.58	6.50	0.59	2.20	ZnPc	0.48	6.20	0.37	1.10	[79]
					SiPc	0.58	7.90	0.59	2.70	
P3HT:$PC_{61}BM$	0.55	8.96	0.71	3.50	SiPc:SiNc	0.57	10.90	0.69	4.30	[80]
P3HT:$PC_{61}BM$	0.58	7.00	0.65	2.64	Aza-BODIPY	0.56	7.85	0.65	2.81	[81]
P3HT:$PC_{61}BM$	0.52	4.93	0.40	1.02	CuPc	0.55	5.70	0.46	1.44	[82]
P3HT:N2200	0.45	3.50	0.52	0.82	SiNc10	0.50	5.70	0.50	1.40	[83]
					SiNc6	0.50	4.50	0.54	1.20	
P3HT:$PC_{61}BM$	0.55	10.70	0.64	3.80	SiPcBz6	0.58	13.10	0.60	4.40	[84]
P3HT:$PC_{61}BM$	0.58	7.80	0.51	2.30	VOPcPhO	0.56	13.50	0.45	3.40	[85]
P3HT:$PC_{61}BM$	0.60	6.80	0.70	3.60	Zn-TTBP	0.61	8.10	0.70	4.30	[86]
P3HT:$PC_{61}BM$	0.54	10.52	0.60	3.41	$(HxN_3)_2$-SiPc	0.58	11.42	0.60	3.58	[87]
P3HT:$PC_{61}BM$	0.62	4.97	0.35	0.78	ZnPc-1py	0.45	4.97	0.35	0.78	[88]
P3HT:$PC_{61}BM$	0.53	10.06	0.53	2.84	(3HS)2-SnPc	0.49	9.82	0.50	2.43	[89]
P3HT:$PC_{61}BM$	0.63	6.77	0.52	2.22	BODIPY 1	0.67	9.45	0.54	3.43	[90]
P3HT:$PC_{61}BM$	0.49	7.28	0.40	1.41	Ru(N-P)2 (O-O)	0.56	7.60	0.50	2.12	[91]
P3HT:$PC_{61}BM$	0.56	8.22	0.59	2.73	SiPc-Py-1	0.62	9.84	0.61	3.75	[92]
					SiPc-Py-2	0.62	9.91	0.62	3.79	
					SiPc-Py-3	0.62	9.99	0.61	3.80	
					SiPc-Py-4	0.62	10.29	0.65	4.13	

OSCs: Organic solar cells; PCE: power conversion efficiency.

2.7% with an increased J_{sc} of 7.9 mA/cm^2 and a comparable FF of 0.59. They attributed the improved J_{sc} to the enhanced photocurrent promoted by SiPc.

Part of the photocurrent originated from the photoexcitation of SiPc itself and the rest was ascribed to the increased charge separation induced by SiPc. Notably, only SiPc located at the interface of P3HT:PCBM could contribute to photocurrent generation, which could also be a principle for the selection of photovoltaic materials.

PT:fullerene derivative:fullerene systems

Cheng and coworkers[93] constructed efficient and thermal stable PT-fullerene ternary OSCs via the in situ polymerization of fullerene derivatives. Two fullerene derivatives (PCBSD and PCBS) with different styrene group contents were incorporated into P3HT:$PC_{61}BM$ to manipulate the film morphology. As depicted in Figure 4A, an optimized morphology was acquired after annealing at 110 °C for 10 min and the second annealing stage triggered the in situ polymerization. As shown in Figure 4B, the initial efficiencies of the control P3HT:$PC_{61}BM$ device and P3HT:$PC_{61}BM$:PCBSD (6:5:1) and P3HT:$PC_{61}BM$:PCBS (6:5:1) ternary OSCs were 4.08%, 3.32% and 3.84%, respectively.

The PCE of the P3HT:$PC_{61}BM$ binary system dropped to 0.69% after continuous heating for 25 h, while the efficiencies of all the ternary OSCs were well retained or even increased. It was discovered that the amorphous PCBS and PCBSD reduced the crystallinity and restricted the mobility of $PC_{61}BM$ and suppressed the aggregation of the acceptor under thermal stress. Furthermore, the crystallization behavior of P3HT was almost unchanged during the first stage of annealing, while the order of P3HT was significantly reduced after annealing at 150 °C.

Lai *et al.* synthesized a series of $PC_{61}BM$ derivatives containing different thiophene units, namely, PCBTE, PCBBTE and PCBTTE, acting as the surfactants for OSCs[94]. Compared with the control P3HT:$PC_{61}BM$, the ternary blends exhibited reduced surface energy and enhanced interfacial adhesion. The champion PCE of 4.37% was achieved by ternary OSCs with 5% PCBTTE content, as shown in Figure 4C. The improved efficiency could be ascribed to the enhanced absorption coefficient originating from the increased order of the P3HT polymer chains. Moreover, ternary OSCs with a 10% PCBTTE content maintained 94% of their initial efficiency after annealing at 150 °C for 10 h, which was much higher than that of the binary system (74%) [Figure 4D]. The authors attributed the improved thermal stability to the suppressed $PC_{61}BM$ aggregation. Apart from functionalized fullerene derivatives, ICBA is another widely used fullerene acceptor. Khlyabich *et al.* demonstrated that the V_{oc} of P3HT:$PC_{61}BM$:ICBA was not determined by the smallest V_{oc} of the corresponding binary systems but could be tuned by varying the weight ratio of the two acceptors[95]. The PCEs of the P3HT:$PC_{61}BM$ and P3HT:ICBA binary systems were 3.57% and 3.98%, respectively, and the V_{oc} of the ternary system increased from 0.605 to 0.844 V, with the ICBA content increased from 0 to 1, as shown in Figure 4E. In addition, all the blend systems achieved comparable FFs, illustrating the balanced charge separation and transport.

PT:donor polymer:fullerene systems

Low bandgap polymers with extended absorption to the near-infrared region are also promising candidates for promoting photocurrent generation. Koppe *et al.* investigated the mechanism of enhanced photosensitivity using a series of characterization methods[96]. They found that the absorption of the blend extended with increasing PCPDTBT fraction, while the film morphology was almost unchanged after annealing. Ternary OSCs with 20% PCPDTBT gave the highest PCE. Neither the energy transfer nor the charge transfer was responsible for the increased J_{sc}. The photoinduced charge transfer from PCPDTBT to P3HT and from PCPDTBT to $PC_{61}BM$ via the P3HT and $PC_{61}BM$ matrices, respectively, was the dominant process, as shown in Figure 5A. Li and coworkers[97] investigated the phase diagram of binary and ternary OSCs based on P3HT:$PC_{61}BM$ and P3HT:PCPDTBT:$PC_{61}BM$, respectively, by DSC and constructed a thermal-electrical property relationship. Small amounts of (less than 20%) PCPDTBT had no obvious effect on the P3HT:$PC_{61}BM$ phase diagram, while higher contents of PCPDTBT led to decreased crystallinity. Ternary OSCs with the blending ratio around the eutectic of the phase diagram exhibited the highest J_{sc}. Using a combination of DSC, GIWAXS and SCLC analysis, Machui *et al.* further explored the effect of the low bandgap polymer PCPDTBT on the crystallization behavior of the P3HT:$PC_{61}BM$ blend[98]. As shown in Figure 5B, the normalized enthalpy of the PCPDTBT:P3HT blend decreased linearly with increasing

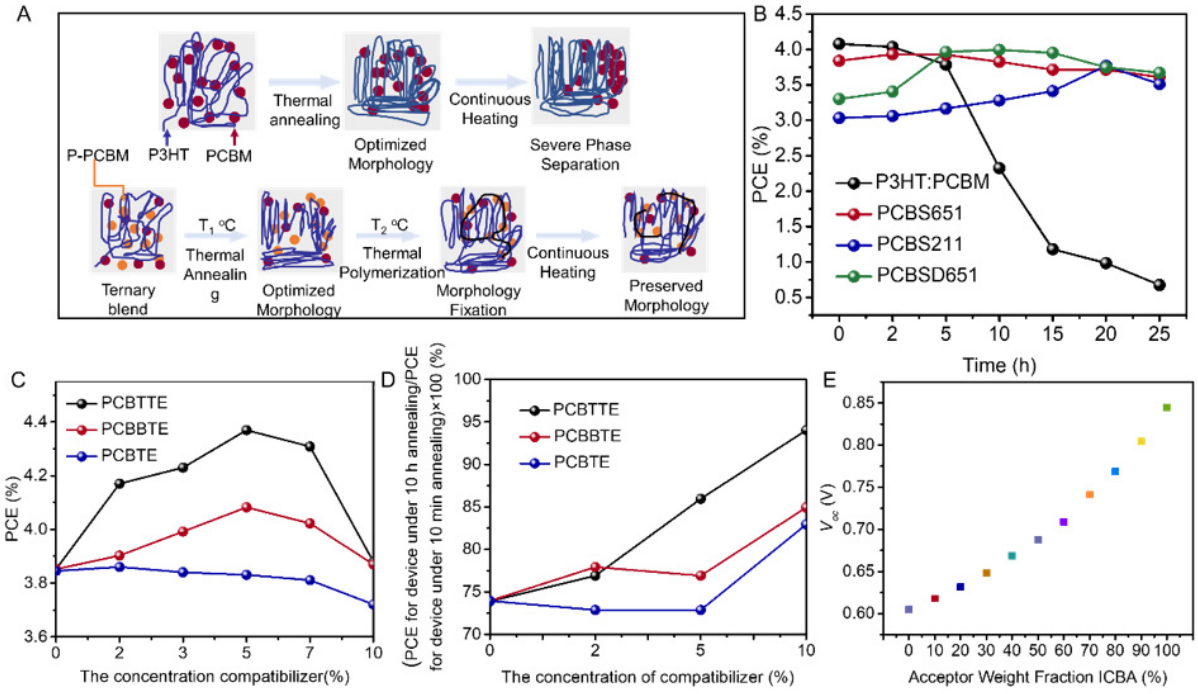

Figure 4. (A) Morphological evolution of P3HT:PC_{61}BM with and without PCBSD or PCBS under thermal stress. (B) PCE of P3HT:PC_{61}BM with different PCBSD or PCBS fractions as a function of annealing time. Reproduced with permission. Copyright, 2011 John Wiley and Sons[93]. (C) PCE and (D) thermal stability of P3HT:PC_{61}BM with different PCBTTE, PCBBTE and PCBTE contents. Reproduced with permission. Copyright, 2011 Elsevier[94]. (E) Variation tendency of *Voc* of P3HT:PC_{61}BM with various ICDA contents. Reproduced with permission. Copyright, 2011 American Chemical Society[95].

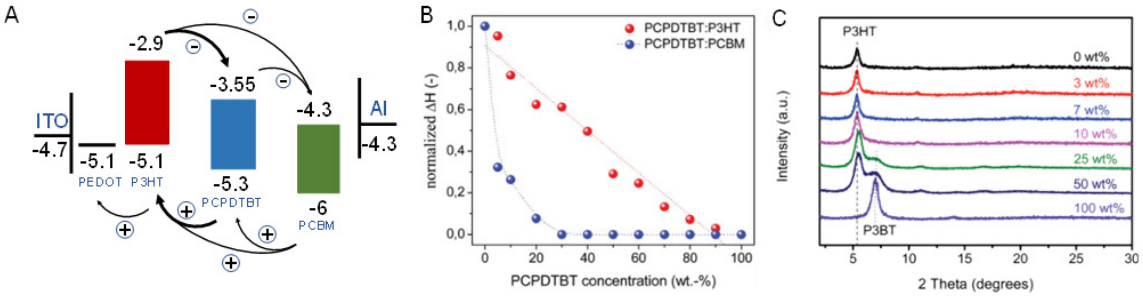

Figure 5. (A) Energy levels of P3HT, PC_{61}BM and PCPDTBT. Reproduced with permission. Copyright, 2010 John Wiley and Sons[96]. (B) Normalized enthalpy of PCPDTBT:P3HT and PCPDTBT:PC_{61}BM blends with various PCPDTBT contents. Reproduced with permission. Copyright, 2012 Royal Society of Chemistry[98]. (C) X-ray spectra of P3HT:PC_{61}BM blends as a function of P3BT content. Reproduced with permission. Copyright, 2015 Royal Society of Chemistry[99].

PCPDTBT content, indicating that PCPDTBT mainly affected the acceptor crystallinity rather than the P3HT ones. Devices with a PCPDTBT content of less than 20% exhibited slightly higher efficiency and a further increase in PCPDTBT content led to a decreased J_{sc} and FF, which was mainly due to the decreased crystallinity of PC_{61}BM.

In addition to low bandgap polymers, P3BT nanowires were also incorporated into the P3HT:PC_{61}BM blend to modulate the film morphology by Zhang and colleagues[99]. Compared with P3BT, the P3BT nanowires demonstrated higher crystallinity and a significantly interconnected structure. As expected, the intensity of the diffraction peaks increased with P3BT nanowire content increasing from 0 to 10%, as shown in

Figure 5C. Moreover, the intensity of the absorption peaks at 605 and 550 nm corresponding to the 0-0 and 0-1 transfers of P3HT, respectively, was significantly enhanced after introducing 10% P3BT nanowires. Consequently, a ternary blend with 7% P3BT nanowires achieved the highest efficiency of 4.2%, which could be ascribed to the increased charge transport pathways provided by the P3HT crystalline phase and $PC_{61}BM$ phase segregation.

PT:NON-FULLERENE-BASED TERNARY OSCS

Non-fullerene acceptors play a critical role in promoting the efficiency of OSCs. Research based on PT:non-fullerene mainly focuses on the classical P3HT:O-IDTBR blend. Baran and coworkers[100] demonstrated highly efficient and thermal stable OSCs by optimizing the ratio of the two non-fullerene acceptors, O-IDTBR and O-IDFBR. The O-IDFBR dispersed in the crystalline P3HT and O-IDTBR phases was favorable for the preservation of the three-phase microstructure and the generation of photocurrent, contributing to increased device performance. Consequently, ternary OSCs based on P3HT:O-IDTBR:O-IDFBR gave a champion PCE of 7.7%. Furthermore, the efficiency of ternary OSCs could be well retained either in air or under illumination [Figure 6A and B].

Furthermore, improving the crystalline phase of the donor and acceptor is another effective method to facilitate charge transport. Liang *et al.*, for example, optimized the crystallinity and vertical phase separation of P3HT:O-IDTBR by separating the crystallization process with a high boiling point solvent (1,2,4-triclorobenzene)[101]. Recently, Liang and colleagues[102] demonstrated a novel method to simultaneously extend the coherence lengths of both P3HT and O-IDTBR by mixing P3HT with different molecular weights. The low molecular weight P3HT relieved the entanglement of polymer chains, leading to a more ordered structure [Figure 6C]. Furthermore, the addition of lower molecular weight P3HT almost had no effect on the intermixed phase amount due to the excellent miscibility. As a result, the PCE of P3HT:O-IDTBR increased from 7.03% to 7.80%, which is the record value for P3HT:O-IDTBR blends.

Regardless of the various processing methods, the device performance of PT-based OSCs is still much lower than the theoretical value. Yuan and coworkers[103] reported a series of cyano group-substituted PTs with varied fluorination degrees named as P5TCN-Fx. Ternary OSCs based on P5TCN-F25:Y6:$PC_{71}BM$ achieved the highest PCE of 17.2% with a V_{oc} of 0.80 V, a J_{sc} of 27.55 mA/cm^2 and a FF of 0.777, as shown in Figure 6D. This is the present efficiency record for PT OSCs and represents a milestone in the field. Recently, Jeong *et al.* developed two fluorinated PT derivatives, PT-2F and PT-4F[104]. The highest occupied molecular orbital energy levels of PT were effectively downshifted due to the strong electron-withdrawing property of fluorine. Furthermore, the incorporation of fluorine enhanced the rigidity and planarity of the backbone, affording PT with improved crystallinity. Compared with PT-2F, PT-4F demonstrated an intense aggregation degree and distinct preaggregation behavior. Benefiting from the optimized morphology, the PT-4F-based devices demonstrated higher charge generation efficiency and the ternary OSCs based on PT-4F:BTP-eC9:L8-BO achieved a PCE of 16.4% with a V_{oc} of 0.842 V, a J_{sc} of 25.27 mA/cm^2 and a FF of 0.77, as shown in Figure 6E. Overall, PT derivatives demonstrate excellent potential for the realization of high-efficiency and low-cost OSCs.

PT AS AN ADDITIVE FOR OSCS

In addition to the above circumstances, PT and its derivatives can also be incorporated into other systems as guest materials to manipulate phase separation and charge transport. For example, Lin *et al.* demonstrated an improved device performance of Si-PCPDTBT:$PC_{71}BM$ by introducing small amounts of P3HT[105]. They found that a blend with 1% P3HT had an enhanced absorption in the range of 375-575 nm, which was complementary to the Si-PCPDTBT:$PC_{71}BM$ blend. Furthermore, the addition of P3HT led to increased

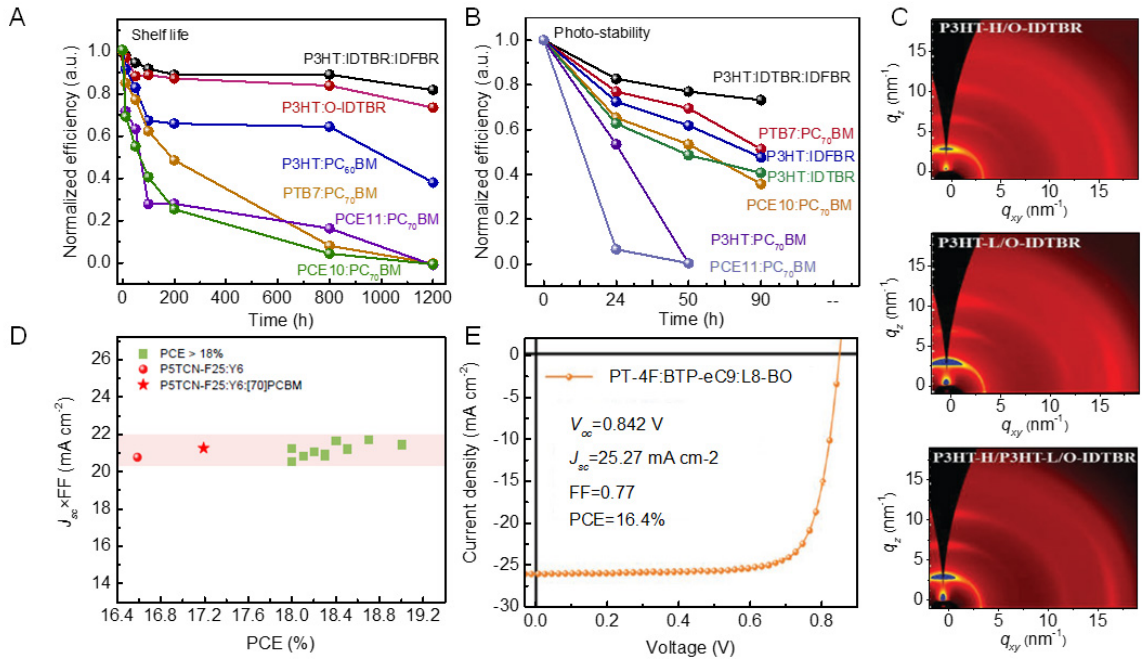

Figure 6. Normalized PCE of P3HT:IDTBR:IDFBR blend and other polymer:fullerene systems as a function of (A) storage and (B) illumination time. Reproduced with permission. Copyright, 2017 Macmillan Publishers Limited, part of Springer Nature[100]. (C) Two-dimensional grazing incidence wide-angle X-ray scattering (GIWAXS) patterns of P3HT-L:P3HT-H:O-IDTBR and ternary OSCs. Reproduced with permission. Copyright, 2021 John Wiley and Sons[102]. (D) *Jsc* × FF as a function of PCE of OSCs based on P5TCN-F25 and other OSCs with PCE >18% in the literature. Reproduced with permission. Copyright, 2022 Elsevier[103]. (E) *J-V* characteristic curve of PT-4F:BTP-eC9:L8-BO. Reproduced with permission. Copyright, 2022 John Wiley and Sons[104].

crystalline size and more significant phase separation [Figure 7A]. Despite the fact that the P3HT dispersed in the blend as the recombination centers led to increased charge recombination, the device performance of the control blend was finally increased due to the simultaneously improved J_{sc} and FF.

Studies have demonstrated that P3HT could replace conventional additives to control the film morphology and crystalline behavior of PTB7-based OSCs. Goh and coworkers[106] reported inverted OSCs based on P3HT:PTB7:$PC_{71}BM$ in 2015 for the first time. According to them, the influence resulting from the energy level differences between the two donors could be finely controlled by varying the blending ratios. The photodynamic, photovoltaic and microstructural properties of PTB7:$PC_{71}BM$ with a P3HT weight ratio in the range of 0%-10% were systemically investigated. The J_{sc} of the 5% ternary blend exhibited a remarkable increase due to the extended spectral response and the reduced recombination loss resulting from the enhanced Förster resonance energy transfer, as shown in Figure 7B. However, the FF of the ternary blend decreased rapidly with increasing P3HT weight ratio due to the distinct different orientations of the two donors. Solvent vapor annealing reduced the interfacial resistance, thereby improving the efficiency of the control device from 8.22% to 8.72%.

When acting as hole-cascade materials, PT and its derivatives can provide additional charge transport pathways via a bridging effect and therefore contribute to the improvement of device performance. Sivakumar *et al.* compared the performance of two PCDTBT:P3HT:$PC_{61}BM$ and PCPDTBT:P3HT:$PC_{61}BM$ blends from the perspective of crystalline behavior, optical properties and film morphology[107]. They found that the P3HT fibers in the PCPDTBT:$PC_{61}BM$ blend provided more pathways for charge transport, contributing to the enhanced device performance. For the PCDTBT:$PC_{61}BM$ blend, the addition of P3HT

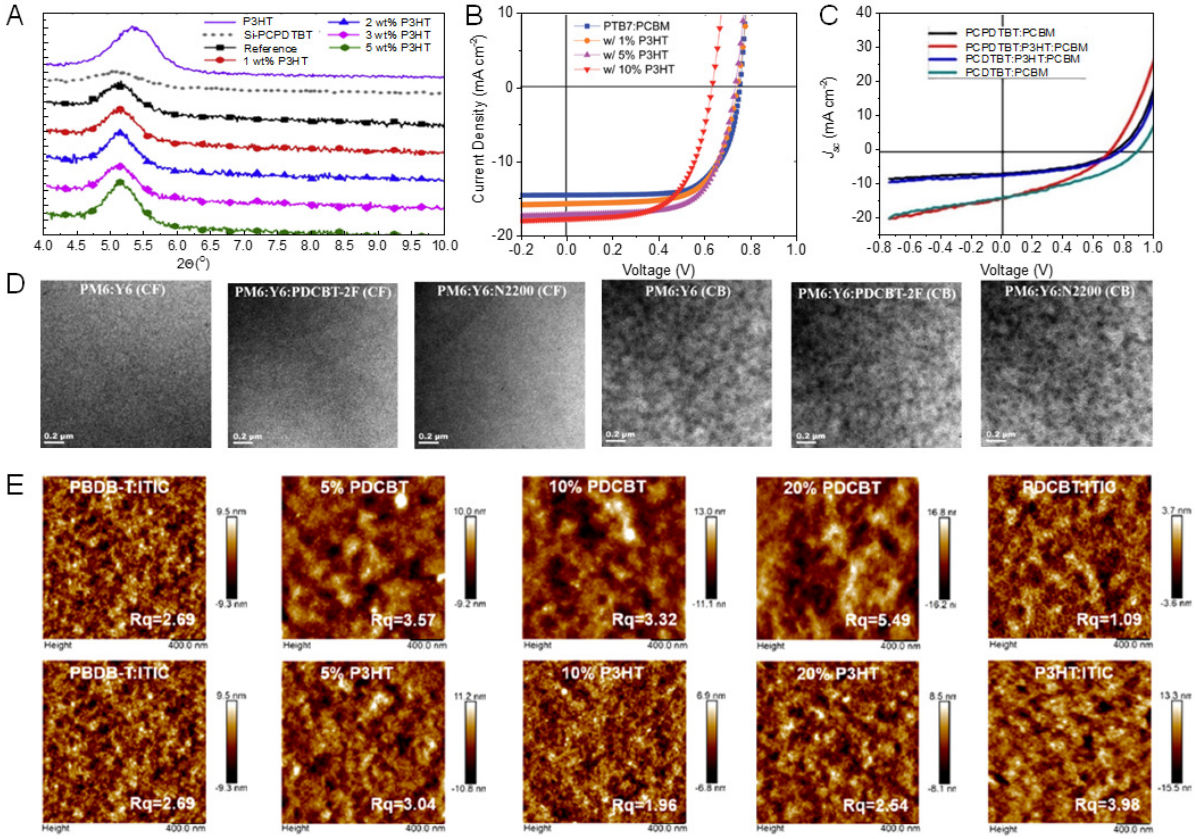

Figure 7. (A) XRD patterns of P3HT and Si-PCPDTBT neat films and blends with various P3HT contents. Reproduced with permission. Copyright, 2014 Elsevier[105]. (B) *J-V* characteristic curves of PTB7:$PC_{71}BM$ with different P3HT contents. Reproduced with permission. Copyright, Royal Society of Chemistry[106]. (C) *J-V* characteristic of PCDTBT:$PC_{61}BM$ with different P3HT contents. Reproduced with permission. Copyright, Elsevier[107]. (D) TEM images of PM6:Y6 binary and PM6:Y6:PDCBT-2F:N2200 ternary blends in CF and CB. Reproduced with permission. Copyright, 2022 American Chemical Society[108]. (E) AFM images of PBDB-T:ITIC as a function of PDCBT and P3HT content. Reproduced with permission. Copyright, 2019 American Chemical Society[109].

had no obvious positive effect on the absorption spectra and the decreased V_{oc} and J_{sc} led to a decreased PCE [Figure 7C].

Based on the understanding that the crystalline state affecting the miscibility of the components might be related to the solvent type used in device fabrication, Yao *et al.* incorporated PDCBT-2F and N2200, acting as the additives, into the PM6:Y6 model system with chloroform (CF) and chlorobenzene (CB) as the processing solvents[108]. They found that the efficiency of the two systems processed with CF had an obvious increase. Different from PM6:Y6:N2200, the PCE of PDCBT-2F:PM6:Y6 processed with CB decreased rapidly due to the mismatched miscibility. As shown in Figure 7D, the excessive phase separation of PDCBT-2F:PM6:Y6 processed with CB led to a decreased PCE, while the incorporation of N2200 barely changed the morphology of the PM6:Y6 films, indicating that the crystallization and miscibility of Y6-based OSCs were related to the preaggregation resulting from the solvent type.

To further investigate the interaction between the third component and the blend from the perspective of miscibility, Yi and coworkers[109] selected two materials with similar chemical structures but different side chains, namely, P3HT and PDCBT, to act as the third component of the PBDB-T:ITIC blend. It was discovered that the miscibility between the third component and the acceptor, instead of the interaction

between P3HT/PDCBT and the polymer donor, dominated the phase separation. The Flory-Huggins interaction parameters of the three PDCBT:PBDB-T, PBDB-T:ITIC and P3HT:PDCBT blends were calculated according to the melting point depression method to evaluate the interaction of different blends. Compared with P3HT:ITIC, PDCBT:ITIC exhibited poor miscibility. Benefiting from the proper phase separation and enhanced crystallization, the device performance based on PDCBT:PBDB-T:ITIC OSCs improved from 9.40% to 10.97% [Figure 7E]. The PCE of P3HT:PBDB-T:ITIC decreased rapidly with increasing P3HT weight ratio. Combined with the previous studies from the same authors, a conclusion was reached that the mechanisms affecting the interaction between the third component and the control blend of OSCs based on fullerene and non-fullerene acceptors are not the same.

It seems that the incorporation of the third component as an additive generally leads to an increased J_{sc} resulting from the complementary absorption between the third component and host materials but a decreased FF originating from the poor compatibility. The film morphology of the ternary OSCs can be well controlled by manipulating the weight ratio of the additives and an appropriate post-treatment. The miscibility induced by the third component type or the preaggregation in different solvents provides guidelines for the selection of guest materials.

CONCLUSIONS AND OUTLOOK

The design of PT and its derivatives boosts the efficiency of PT-based OSCs to over 17%. Ternary mixing is an effective strategy for further improving the efficiency and stability of PT-based OSCs. Applying approaches employed in fullerene OSCs may be an effective route to achieving highly efficient and thermally stable OSCs for PT:nonfullerene. Insulating polymers, conjugated small molecules and donor polymers are the most widely used guest materials. Notably, some studies have demonstrated that insulating polymers not only can effectively enhance the device performance, thermal stability[110] and mechanical properties of OSCs, but can also be conveniently applied in different systems[111]. Therefore, more emphasis should be devoted to the insulating polymers involved in ternary OSCs. Despite several principles based on absorption, energy levels, miscibility and the glass transition temperature having been proposed, specific and universal criteria should be perfected for selecting appropriate third components efficiently. Finally, we outline herein five possible directions that deserve further attention.

(1) Thermally stable PT-based ternary solar cells

Excellent thermal stability is a prerequisite for the practical application of OSCs. Several studies have demonstrated that the morphology of blend systems containing appropriate third components, such as photovoltaic materials or insulating polymers, with good compatibility with host materials can be stabilized under continuous heating, contributing to the well-retained efficiency. As a small change in side chains can make a remarkable difference to its properties, PT can behave differently when the side chain is varied, for instance, odd or even numbered carbon chains. Blending two different PTs[112,113] is very promising for achieving thermally stable and high-efficiency solar cells. Furthermore, applying high-T_g insulators[114] might be another good option.

(2) Mechanically robust PT-based all-polymer ternary solar cells

Flexible and stretchable OSCs with high efficiency and excellent mechanical stability are considered as the most promising powering sources for wearable electronic devices. Li *et al.* recently demonstrated over 7% efficiency in all-polymer solar cells based on P3HT[115]. Thus, constructing ternary blends might be an efficient means to obtain over 10% efficiency in this kind of solar cell. Moreover, the cells might be

mechanically stretchable due to the entanglement of PT and polymer acceptors[2,116-118]. In addition, combining ternary blends with flexible substrates, such as flexible conductive textiles, is an effective strategy for achieving wearable electronic devices.

(3) High-efficiency PT/quantum dot hybrid solar cells

A recent study[119] has shown the significant potential of polythiophenes in achieving high-performance hybrid organic and quantum dot solar cells[120,124]. Thus, designing ternary blends comprising PT as hole transporting layers might promote the power conversion efficiency of hybrid solar cells greatly.

(4) Low-cost OSCs in real applications

Despite the scalability of PT and its derivatives, the high cost of acceptor molecules with highly fused and large aromatic groups seriously hinders the commercial application of OSCs. Therefore, the design and synthesis of acceptors with simple chemical structures and good reproducibility, such as non-fused ring acceptors based on oligothiophenes and derivatives, is urgently required.

(5) Large-area OSCs based on PT

Studies have demonstrated that the insulators involved in ternary blends with varied film thicknesses can achieve comparable performance, which is favorable for the large-scale application of OSCs. Nonetheless, the relatively low efficiency is still the main challenge OSCs face. The ternary mixing of PT derivatives and insulator polymers may be a feasible method to fabricate high-efficiency large-area OSCs via scalable coating techniques such as blade-coating, slot-die coating, and roll-to-roll printing.

DECLARATIONS

Authors' contributions

Made substantial contributions to conception and design of the study: Ye L
Performed literature survey and wrote the first draft: Qi Q
Performed manuscript revisions, as well as provided administrative and technical support: Ye L, Ke H

Availability of data and materials

Not applicable.

Financial support and sponsorship

This work was supported by the Natural Science Foundation of Fujian Province (No. 2022J011131), the Open Fund of Fujian Key Laboratory of Electrochemical Energy Storage Materials, Fuzhou University (No. 2021CN02), and Fundamental Research Funds for the Central Universities. Ye L also appreciated the Peiyang Scholar Program of Tianjin University for support.

Conflicts of interest

All authors declared that there are no conflicts of interest.

Ethical approval and consent to participate

Not applicable.

Consent for publication

Not applicable.

REFERENCES

1. Wu J, Gao M, Chai Y, et al. Towards a bright future: the versatile applications of organic solar cells. *Mater Rep Energy* 2021;1:100062. DOI
2. Zhou K, Xian K, Qi Q, et al. Unraveling the correlations between mechanical properties, miscibility, and film microstructure in all-polymer photovoltaic cells. *Adv Funct Mater* 2022;32:2201781. DOI
3. Wu Y, Kong J, Qin Y, et al. Realizing green solvent processable non-fullerene organic solar cells by modulating the side groups of conjugated polymers. *Acta Phys Chim Sin* 2019;35:1391-1398. DOI
4. Zhang W, Huang J, Lv X, et al. Chlorinated phthalimide polymer donor as ultra-wide bandgap and deep HOMO guest for achieving highly eficient polymer solar cells. *Chin Chem Lett* 2022. DOI
5. Wang H, Lu H, Chen YN, et al. Chlorination enabling a low-cost benzodithiophene-based wide-bandgap donor polymer with an efficiency of over 17. *Adv Mater* 2022;34:e2105483. DOI PubMed
6. Zhu L, Zhang M, Xu J, et al. Single-junction organic solar cells with over 19% efficiency enabled by a refined double-fibril network morphology. *Nat Mater* 2022;21:656-63. DOI PubMed
7. Wei Y, Chen Z, Lu G, et al. Binary organic solar cells breaking 19% via Manipulating the vertical component distribution. *Adv Mater* 2022;34:e2204718. DOI PubMed
8. Sun R, Wu Y, Yang X, et al. Single-junction organic solar cells with 19.17% efficiency enabled by introducing one asymmetric guest acceptor. *Adv Mater* 2022;34:e2110147. DOI PubMed
9. Cui Y, Xu Y, Yao H, et al. Single-junction organic photovoltaic cell with 19% efficiency. *Adv Mater* 2021;33:e2102420. DOI PubMed
10. Liu Y, Liu B, Ma C, et al. Recent progress in organic solar cells (part II device engineering). *Sci China Chem* 2022;65:1457-97. DOI
11. Liu Y, Liu B, Ma C, et al. Recent progress in organic solar cells (part I material science). *Sci China Chem* 2022;65:224-68. DOI
12. Yang M, Wei W, Zhou X, Wang Z, Duan C. Non-fused ring acceptors for organic solar cells. *Energy Mater* 2022;1:100008. DOI
13. Ye L, Ke H, Liu Y. The renaissance of polythiophene organic solar cells. *Trends Chem* 2021;3:1074-87. DOI
14. Mehmood U, Al-ahmed A, Hussein IA. Review on recent advances in polythiophene based photovoltaic devices. *Renew Sust Energ Rev* 2016;57:550-61. DOI
15. Wadsworth A, Hamid Z, Bidwell M, et al. Progress in poly (3-hexylthiophene) organic solar cells and the influence of its molecular weight on device performance. *Adv Energy Mater* 2018;8:1801001. DOI
16. Yang C, Zhang S, Hou J. Low-cost and efficient organic solar cells based on polythiophene-and poly(thiophene vinylene)-related donors. *Aggregate* 2021;3:e111. DOI
17. Xu X, Wu H, Liang S, et al. Quantum efficiency and voltage losses in P3HT: non-fullerene solar cells. *Acta Phys Chim Sin* 2022;0:2201039-0. DOI
18. Chatterjee S, Jinnai S, Ie Y. Nonfullerene acceptors for P3HT-based organic solar cells. *J Mater Chem A* 2021;9:18857-86. DOI PubMed
19. Zhou D, You W, Xu H, et al. Recent progress in ternary organic solar cells based on solution-processed non-fullerene acceptors. *J Mater Chem A* 2020;8:23096-122. DOI
20. Holliday S, Ashraf RS, Wadsworth A, et al. High-efficiency and air-stable P3HT-based polymer solar cells with a new non-fullerene acceptor. *Nat Commun* 2016;7:11585. DOI PubMed PMC
21. Xu X, Zhang G, Yu L, Li R, Peng Q. P3HT-based polymer solar cells with 8.25% efficiency enabled by a matched molecular acceptor and smart green-solvent processing technology. *Adv Mater* 2019;31:e1906045. DOI PubMed
22. Yang C, Zhang S, Ren J, et al. Molecular design of a non-fullerene acceptor enables a P3HT-based organic solar cell with 9.46% efficiency. *Energy Environ Sci* 2020;13:2864-9. DOI
23. Xian K, Liu Y, Liu J, et al. Delicate crystallinity control enables high-efficiency P3HT organic photovoltaic cells. *J Mater Chem A* 2022;10:3418-29. DOI
24. Xian K, Geng Y, Ye L. The rise of polythiophene photovoltaics. *Joule* 2022;6:941-4. DOI
25. Liu Y, Xian K, Zhang X, et al. A mixed-ligand strategy to modulate P3HT regioregularity for high-efficiency solar cells. *Macromolecules* 2022;55:3078-86. DOI
26. Liang Z, Li M, Wang Q, et al. Optimization requirements of efficient polythiophene:nonfullerene organic solar cells. *Joule* 2020;4:1278-95. DOI
27. Gao M, Liu Y, Xian K, et al. Thermally stable poly(3-hexylthiophene): nonfullerene solar cells with efficiency breaking 10%. *Aggregate* 2022:e190. DOI
28. Xu Q, Chang C, Li W, et al. Non-fullerene polymer solar cells based on a new polythiophene derivative as donor. *Acta Phys Chim Sin*

2019;35:268-274. DOI
29. Zhang M, Guo X, Ma W, Ade H, Hou J. A polythiophene derivative with superior properties for practical application in polymer solar cells. *Adv Mater* 2014;26:5880-5. DOI PubMed
30. Qin Y, Uddin MA, Chen Y, et al. Highly efficient fullerene-free polymer solar cells fabricated with polythiophene derivative. *Adv Mater* 2016;28:9416-22. DOI PubMed
31. Zhang H, Li S, Xu B, Yao H, Yang B, Hou J. Fullerene-free polymer solar cell based on a polythiophene derivative with an unprecedented energy loss of less than 0.5 eV. *J Mater Chem A* 2016;4:18043-9. DOI
32. Yao H, Qian D, Zhang H, et al. Critical role of molecular electrostatic potential on charge generation in organic solar cells: critical role of molecular electrostatic potential on charge generation in organic solar cells. *Chin J Chem* 2018;36:491-4. DOI
33. Wang Q, Li M, Zhang X, et al. Carboxylate-substituted polythiophenes for efficient fullerene-free polymer solar cells: the effect of chlorination on their properties. *Macromolecules* 2019;52:4464-74. DOI
34. Wang Q, Li M, Peng Z, et al. Calculation aided miscibility manipulation enables highly efficient polythiophene:nonfullerene photovoltaic cells. *Sci China Chem* 2021;64:478-87. DOI
35. Jia X, Chen Z, Duan C, et al. Polythiophene derivatives compatible with both fullerene and non-fullerene acceptors for polymer solar cells. *J Mater Chem C* 2019;7:314-23. DOI
36. Jia X, Liu G, Chen S, et al. Backbone fluorination of polythiophenes improves device performance of non-fullerene polymer solar cells. *ACS Appl Energy Mater* 2019;2:7572-83. DOI
37. Yuan X, Zhao Y, Zhang Y, et al. Achieving 16% efficiency for polythiophene organic solar cells with a cyano-substituted polythiophene. *Adv Funct Mater* 2022;32:2201142. DOI
38. Liu W, Lu H, Zhang Y, et al. Enhancing the performance of organic solar cells by modification of cathode with a self-assembled monolayer of aromatic organophosphonic acid. *Chin Chem Lett* 2022. DOI
39. Xue P, Zhang J, Xin J, et al. Effects of terminal groups in third components on performance of organic solar cells. *Acta Phys Chim Sin* 2019;35:275-283. DOI
40. Xu W, Gao F. The progress and prospects of non-fullerene acceptors in ternary blend organic solar cells. *Mater Horiz* 2018;5:206-21. DOI
41. Xu X, Li Y, Peng Q. Ternary blend organic solar cells: understanding the morphology from recent progress. *Adv Mater* 2021;33:e2107476. DOI PubMed
42. Lu L, Kelly MA, You W, Yu L. Status and prospects for ternary organic photovoltaics. *Nat Photon* 2015;9:491-500. DOI
43. Wang Y, Zhuang C, Fang Y, Yu H, Wang B. Various roles of dye molecules in organic ternary blend solar cells. *Dyes Pigment* 2020;176:108231. DOI
44. Wang J, Ye L. When electronically inert polymers meet conjugated polymers: emerging opportunities in organic photovoltaics. *Chin J Polym Sci* 2022;40:861-9. DOI
45. Li H, Lu K, Wei Z. Polymer/small molecule/fullerene based ternary solar cells. *Adv Energy Mater* 2017;7:1602540. DOI
46. Lu H, Xu X, Bo Z. Perspective of a new trend in organic photovoltaic: ternary blend polymer solar cells. *Sci China Mater* 2016;59:444-58. DOI
47. Gao M, Wang W, Hou J, Ye L. Control of aggregated structure of photovoltaic polymers for high-efficiency solar cells. *Aggregate* 2021;2:e46. DOI
48. Gao M, Liang Z, Geng Y, Ye L. Significance of thermodynamic interaction parameters in guiding the optimization of polymer:nonfullerene solar cells. *Chem Commun* 2020;56:12463-78. DOI PubMed
49. Liu J, Xian K, Ye L, Zhou Z. Open-circuit voltage loss in lead chalcogenide quantum dot solar cells. *Adv Mater* 2021;33:e2008115. DOI PubMed
50. Park E, Fu H, Choi M, Luan W, Kim Y. Effects of ligand-exchanged cadmium selenide nanoparticles on the performance of P3HT:PCBM:CdSe ternary system solar cells. *Bull Korean Chem Soc* 2013;34:2321-4. DOI
51. Zhao S, Pi X, Mercier C, Yuan Z, Sun B, Yang D. Silicon-nanocrystal-incorporated ternary hybrid solar cells. *Nano Energy* 2016;26:305-12. DOI
52. Fan W, Li H, Zhang H, et al. Study on the influence of embedded structure of carbon quantum dots of the organic solar cells with the territory active layer structure of P3HT: PC61BM: CQDs. *J Mater Sci Mater Electron* 2021;32:2293-301. DOI
53. Yoon S, Heo SJ, Kim HJ. Hybrid polymer/inorganic nanoparticle blended ternary solar cells: Hybrid polymer/inorganic nanoparticle blended ternary solar cells. *Phys Status Solidi RRL* 2013;7:534-7. DOI
54. Gebhardt RS, Du P, Peer A, et al. Utilizing wide band gap, high dielectric constant nanoparticles as additives in organic solar cells. *J Phys Chem C* 2015;119:23883-9. DOI
55. Nam M, Kim S, Kang M, Kim S, Lee K. Efficiency enhancement in organic solar cells by configuring hybrid interfaces with narrow bandgap PbSSe nanocrystals. *Org Electron* 2012;13:1546-52. DOI
56. Ongul F, Yuksel SA, Allahverdi C, Bozar S, Kazici M, Gunes S. Influences of CdSe NCs on the photovoltaic parameters of BHJ organic solar cells. *Spectrochim Acta A Mol Biomol Spectrosc* 2018;194:50-6. DOI PubMed
57. Sung SJ, Kim JH, Gihm SH, et al. Revisiting the role of graphene quantum dots in ternary organic solar cells: insights into the nanostructure reconstruction and effective förster resonance energy transfer. *ACS Appl Energy Mater* 2019;2:8826-35. DOI
58. Yousaf S, Ikram M, Ali S. Compositional engineering of acceptors for highly efficient bulk heterojunction hybrid organic solar cells. *J Colloid Interface Sci* 2018;527:172-9. DOI

59. Wu W, Wu H, Zhong M, Guo S. Dual role of graphene quantum dots in active layer of inverted bulk heterojunction organic photovoltaic devices. *ACS Omega* 2019;4:16159-65. DOI PubMed PMC
60. Lefrançois A, Luszczynska B, Pepin-Donat B, et al. Enhanced charge separation in ternary P3HT/PCBM/CuInS2 nanocrystals hybrid solar cells. *Sci Rep* 2015;5:7768. DOI PubMed PMC
61. Al-busaidi Z, Pearson C, Groves C, Petty MC. Enhanced lifetime of organic photovoltaic diodes utilizing a ternary blend including an insulating polymer. *Sol Energy Mater Sol Cells* 2017;160:101-6. DOI
62. Kumano M, Ide M, Seiki N, Shoji Y, Fukushima T, Saeki A. A ternary blend of a polymer, fullerene, and insulating self-assembling triptycene molecules for organic photovolatics. *J Mater Chem A* 2016;4:18490-8. DOI
63. Chen F, Chien S. Nanoscale functional interlayers formed through spontaneous vertical phase separation in polymer photovoltaic devices. *J Mater Chem* 2009;19:6865. DOI
64. Wang H, Zhang W, Xu C, Bi X, Chen B, Yang S. Efficiency enhancement of polymer solar cells by applying poly(vinylpyrrolidone) as a cathode buffer layer via spin coating or self-assembly. *ACS Appl Mater Interfaces* 2013;5:26-34. DOI
65. Yao K, Chen L, Chen X, Chen Y. Self-organized hole transport layers based on polythiophene diblock copolymers for inverted organic solar cells with high efficiency. *Chem Mater* 2013;25:897-904. DOI
66. Yu L, Li C, Li Q, et al. Performance improvement of conventional and inverted polymer solar cells with hydrophobic fluoropolymer as nonvolatile processing additive. *Org Electron* 2015;23:99-104. DOI
67. Yamakawa S, Tajima K, Hashimoto K. Buffer layer formation in organic photovoltaic cells by self-organization of poly(dimethylsiloxane)s. *Org Electron* 2009;10:511-4. DOI
68. Ferenczi TA, Müller C, Bradley DD, Smith P, Nelson J, Stingelin N. Organic semiconductor: insulator polymer ternary blends for photovoltaics. *Adv Mater* 2011;23:4093-7. DOI PubMed
69. Dauzon E, Sallenave X, Plesse C, Goubard F, Amassian A, Anthopoulos TD. Versatile methods for improving the mechanical properties of fullerene and non-fullerene bulk heterojunction layers to enable stretchable organic solar cells. *J Mater Chem C* 2022;10:3375-86. DOI
70. Zhang K, Bi P, Wen Z, et al. Unveiling the important role of non-fullerene acceptors crystallinity on optimizing nanomorphology and charge transfer in ternary organic solar cells. *Org Electron* 2018;62:643-52. DOI
71. Cheng P, Shi Q, Zhan X. Ternary blend organic solar cells based on P3HT/TT-TTPA/PC $_{61}$ BM. *Acta Chim Sinica* 2015;73:252. DOI
72. Bi PQ, Wu B, Zheng F, et al. An obvious improvement in the performance of ternary organic solar cells with "Guest" donor present at the "Host" donor/acceptor interface. *ACS Appl Mater Interfaces* 2016;8:23212-21. DOI PubMed
73. Galli D, Gasparini N, Forster M, et al. Suppressing the surface recombination and tuning the open-circuit voltage of polymer/fullerene solar cells by implementing an aggregative ternary compound. *ACS Appl Mater Interfaces* 2018;10:28803-11. DOI PubMed
74. Mohapatra AA, Kim V, Puttaraju B, et al. Förster resonance energy transfer drives higher efficiency in ternary blend organic solar cells. *ACS Appl Energy Mater* 2018;1:4874-82. DOI
75. Wang Y, Wang T, Chen J, et al. Quadrupolar D-A-D diketopyrrolopyrrole-based small molecule for ternary blend polymer solar cells. *Dyes Pigment* 2018;158:213-8. DOI
76. Matsumoto K, Yamashita K, Sakoda Y, et al. Organic thin-film solar cells using benzotrithiophene derivatives bearing acceptor units as non-fullerene acceptors. *Eur J Org Chem* 2021;2021:4620-9. DOI
77. Lim E. The effects of molecular packing behavior of small-molecule acceptors in ternary organic solar cells. *Appl Sci* 2021;11:755. DOI
78. Fu P, Yang D, Zhang F, Yu W, Zhang J, Li C. Efficiency enhancement of P3HT:PCBM polymer solar cells using oligomers DH4T as the third component. *Sci China Chem* 2015;58:1169-75. DOI
79. Honda S, Nogami T, Ohkita H, Benten H, Ito S. Improvement of the light-harvesting efficiency in polymer/fullerene bulk heterojunction solar cells by interfacial dye modification. *ACS Appl Mater Interfaces* 2009;1:804-10. DOI PubMed
80. Honda S, Ohkita H, Benten H, Ito S. Multi-colored dye sensitization of polymer/fullerene bulk heterojunction solar cells. *Chem Commun* 2010;46:6596-8. DOI PubMed
81. Min J, Ameri T, Gresser R, et al. Two similar near-infrared (IR) absorbing benzannulated aza-BODIPY dyes as near-IR sensitizers for ternary solar cells. *ACS Appl Mater Interfaces* 2013;5:5609-16. DOI PubMed
82. Derouiche H, Mohamed AB. Thermal annealing effect on poly(3-hexylthiophene): fullerene:copper-phthalocyanine ternary photoactive layer. *Sci World J* 2013;2013:914981. DOI PubMed PMC
83. Xu H, Ohkita H, Hirata T, Benten H, Ito S. Near-IR dye sensitization of polymer blend solar cells. *Polymer* 2014;55:2856-60. DOI
84. Xu H, Ohkita H, Tamai Y, Benten H, Ito S. Interface engineering for ternary blend polymer solar cells with a heterostructured near-IR dye. *Adv Mater* 2015;27:5868-74. DOI PubMed
85. Ahmad Z, Touati F, Shakoor RA, Al-thani NJ. Study of a ternary blend system for bulk heterojunction thin film solar cells. *Chinese Phys B* 2016;25:080701. DOI
86. Keawsongsaeng W, Gasiorowski J, Denk P, et al. Systematic investigation of porphyrin-thiophene conjugates for ternary bulk heterojunction solar cells. *Adv Energy Mater* 2016;6:1600957. DOI
87. Grant TM, Gorisse T, Dautel O, Wantz G, Lessard BH. Multifunctional ternary additive in bulk heterojunction OPV: increased device performance and stability. *J Mater Chem A* 2017;5:1581-7. DOI
88. Kadem B, Kaya EN, Hassan A, Durmuş M, Basova T. Composite materials of P3HT:PCBM with pyrene substituted zinc(II)

phthalocyanines: characterisation and application in organic solar cells. *Solar Energy* 2019;189:1-7. DOI
89. Grant TM, Rice NA, Muccioli L, Castet F, Lessard BH. Solution-processable n-type tin phthalocyanines in organic thin film transistors and as ternary additives in organic photovoltaics. *ACS Appl Electron Mater* 2019;1:494-504. DOI
90. Wanwong S, Sangkhun W, Kumnorkaew P, Wootthikanokkhan J. Improved performance of ternary solar cells by using BODIPY triads. *Materials* 2020;13:2723. DOI PubMed PMC
91. Akel S, Sharif MA, Al-esseili R, et al. Photovoltaic cells based on ternary P3HT:PCBM: Ruthenium(II) complex bearing 8-(diphenylphosphino)quinoline active layer. *Colloids Surf A Physicochem Eng Asp* 2021;622:126685. DOI
92. Ke L, Min J, Adam M, et al. A series of pyrene-substituted silicon phthalocyanines as near-ir sensitizers in organic ternary solar cells. *Adv Energy Mater* 2016;6:1502355. DOI
93. Cheng Y, Hsieh C, Li P, Hsu C. Morphological stabilization by in situ polymerization of fullerene derivatives leading to efficient, thermally stable organic photovoltaics. *Adv Funct Mater* 2011;21:1723-32. DOI
94. Lai Y, Higashihara T, Hsu J, Ueda M, Chen W. Enhancement of power conversion efficiency and long-term stability of P3HT/PCBM solar cells using C60 derivatives with thiophene units as surfactants. *Sol Energy Mater Sol Cells* 2012;97:164-70. DOI
95. Khlyabich PP, Burkhart B, Thompson BC. Efficient ternary blend bulk heterojunction solar cells with tunable open-circuit voltage. *J Am Chem Soc* 2011;133:14534-7. DOI PubMed
96. Koppe M, Egelhaaf H, Dennler G, et al. Near IR sensitization of organic bulk heterojunction solar cells: towards optimization of the spectral response of organic solar cells. *Adv Funct Mater* 2010;20:338-46. DOI
97. Li N, Machui F, Waller D, Koppe M, Brabec CJ. Determination of phase diagrams of binary and ternary organic semiconductor blends for organic photovoltaic devices. *Sol Energy Mater Sol Cells* 2011;95:3465-71. DOI
98. Machui F, Rathgeber S, Li N, Ameri T, Brabec CJ. Influence of a ternary donor material on the morphology of a P3HT:PCBM blend for organic photovoltaic devices. *J Mater Chem* 2012;22:15570. DOI
99. Zhang L, Zhou W, Shi J, et al. Poly(3-butylthiophene) nanowires inducing crystallization of poly(3-hexylthiophene) for enhanced photovoltaic performance. *J Mater Chem C* 2015;3:809-19. DOI
100. Baran D, Ashraf RS, Hanifi DA, et al. Reducing the efficiency-stability-cost gap of organic photovoltaics with highly efficient and stable small molecule acceptor ternary solar cells. *Nat Mater* 2017;16:363-9. DOI PubMed
101. Liang Q, Jiao X, Yan Y, et al. Separating crystallization process of P3HT and O-IDTBR to construct highly crystalline interpenetrating network with optimized vertical phase separation. *Adv Funct Mater* 2019;29:1807591. DOI
102. Liang Q, Hu Z, Yao J, et al. Blending donors with different molecular weights: an efficient strategy to resolve the conflict between coherence length and intermixed phase in polymer/nonfullerene solar cells. *Small* 2022;18:e2103804. DOI PubMed
103. Yuan X, Zhao Y, Xie D, et al. Polythiophenes for organic solar cells with efficiency surpassing 17%. *Joule* 2022;6:647-61. DOI
104. Jeong D, Kim G, Lee D, et al. Sequentially fluorinated polythiophene donors for high-performance organic solar cells with 16.4% efficiency. *Adv Energy Mater* 2022;12:2201603. DOI
105. Lin R, Wright M, Chan KH, et al. Performance improvement of low bandgap polymer bulk heterojunction solar cells by incorporating P3HT. *Org Electron* 2014;15:2837-46. DOI
106. Goh T, Huang J, Bartolome B, et al. Panchromatic polymer-polymer ternary solar cells enhanced by Förster resonance energy transfer and solvent vapor annealing. *J Mater Chem A* 2015;3:18611-21. DOI
107. Sivakumar G, Pratyusha T, Shen W, Gupta D. Performance of donor-acceptor copolymer materials PCPDTBT and PCDTBT with poly hexyl thiophene polymer in a ternary blend. *Mater Today* 2017;4:5060-6. DOI
108. Yao G, Ge Y, Xiao X, et al. Preaggregation in solution producing multiple crystal forms of Y6 corresponding to a variation of miscibility in pm6-based ternary solar cells. *ACS Appl Energy Mater* 2022;5:1193-204. DOI
109. Yi N, Ai Q, Zhou W, et al. Miscibility matching and bimolecular crystallization affording high-performance ternary nonfullerene solar cells. *Chem Mater* 2019;31:10211-24. DOI
110. Ye L, Gao M, Hou J. Advances and prospective in thermally stable nonfullerene polymer solar cells. *Sci China Chem* 2021;64:1875-87. DOI
111. Peng Z, Xian K, Cui Y, et al. Thermoplastic elastomer tunes phase structure and promotes stretchability of high-efficiency organic solar cells. *Adv Mater* 2021;33:e2106732. DOI PubMed
112. Liu Y, Xian K, Gui R, et al. Simple polythiophene solar cells approaching 10% efficiency via carbon chain length modulation of poly(3-alkylthiophene). *Macromolecules* 2022;55:133-45. DOI
113. Yang X, Gao M, Bi Z, et al. Unraveling the photovoltaic, mechanical, and microstructural properties and their correlations in simple poly(3-pentylthiophene) solar cells. *Macromol Rapid Commun* 2022:e2200229. DOI PubMed
114. Chen F, Zhang Y, Wang Q, et al. High *Tg* polymer insulator yields organic photovoltaic blends with superior thermal stability at 150 °C. *Chin J Chem* 2021;39:2570-8. DOI
115. Li Y, Zhang Y, Wu B, et al. High-efficiency P3HT-based all-polymer solar cells with a thermodynamically miscible polymer acceptor. *Solar RRL* 2022;6:2200073. DOI
116. Luo Z, Liu T, Ma R, et al. Precisely controlling the position of bromine on the end group enables well-regular polymer acceptors for all-polymer solar cells with efficiencies over 15. *Adv Mater* 2020;32:e2005942. DOI PubMed
117. Li B, Zhang X, Wu Z, et al. Over 16% efficiency all-polymer solar cells by sequential deposition. *Sci China Chem* 2022;65:1157-63. DOI
118. Zhou K, Xian K, Ye L. Morphology control in high-efficiency all-polymer solar cells. *InfoMat* 2022:4. DOI

119. Liu J, Liu Y, Wang J, et al. Brominated polythiophene reduces the efficiency-stability-cost gap of organic and quantum dot hybrid solar cells. *Adv Energy Mater* 2022;12:2201975. DOI
120. Liu J, Qiao J, Zhou K, et al. An aggregation-suppressed polymer blending strategy enables high-performance organic and quantum dot hybrid solar cells. *Small* 2022;18:e2201387. DOI PubMed
121. Kim H, Shin M, Kim Y. Distinct annealing temperature in polymer:fullerene:polymer ternary blend solar cells. *J Phys Chem C* 2009;113:1620-23. DOI
122. Xu ZX, Roy VA, Low KH, Che CM. Bulk heterojunction photovoltaic cells based on tetra-methyl substituted copper(II) phthalocyanine:P3HT:PCBM composite. *Chem Commun* 2011;47:9654-6. DOI
123. Khlyabich PP, Burkhart B, Thompson BC. Compositional dependence of the open-circuit voltage in ternary blend bulk heterojunction solar cells based on two donor polymers. *J Am Chem Soc* 2012;134:9074-7. DOI
124. Wang J, Liu J, Zhou K, et al. Processing poly(3-hexylthiophene) interlayer with non-halogenated solvents for high-performance and low-cost quantum dot solar cells. *Solar RRL* 2022:e2200779. DOI